



The Potential Role of Apparent Diffusion Coefficient Values in the Differentiation of Tuberculous and Malignant Lymph Nodes of Neck - In Correlation with Histopathology

Authors

Dr Rujuta Narendra Rege MD¹, Dr Praveen Sharma MD², Dr Avinash Naikwadi DNB³
Dr Adipudi Renuka MD⁴, Prof. Dr Kulasekaran DMRD MD⁵, Dr C.R. Seena MD DNB⁶

¹3rd Year Post Graduate, ²Assistant Professor, ³Nanavathi Hospital, Mumbai

⁴1st Year Post Graduate, ⁵Professor and Head of Department, ⁶Professor

^{1,2,4,5,6}Saveetha Medical College and Hospital

Corresponding Author

Dr Praveen Sharma MD

Assistant Professor, Saveetha Medical College and Hospital

Abstract

Study was done in 46 patients to ascertain the different causes of cervical lymphadenopathy. 16 patients with cervical lymph node metastasis from head and neck squamous cell carcinomas (SCC), 2 patients with lymphoma, 1 patient with infective etiology and 27 patients with tuberculous lymphadenitis underwent conventional magnetic resonance imaging (MRI) and diffusion-weighted imaging (DWI). The ADC values of necrotic and solid portions of lymph nodes were measured and compared. Receiver operating characteristic (ROC) analysis was employed to investigate whether ADC values could help to distinguish between the causes of cervical lymphadenopathy.

Aims: To assess the role of MRI with the help of DWI and ADC to differentiate tuberculous from malignant lymph nodes.

Objective: To calculate sensitivity, specificity and other statistical parameters in the differentiation of tuberculous and malignant lymph nodes of neck using diffusion weighted imaging (DWI) and apparent diffusion coefficient (ADC) values with histopathological examination as the gold standard.

Methods and Material

Inclusion Criteria:

1. Patients presenting with cervical lymphadenopathy detected either clinically or by other radiological investigations. In case of multiple lymph nodes, largest will be included in the study.
2. Patients who undergo biopsy for the same.

Exclusion Criteria

1. Patients with cervical lymph node of size less than 15mm in short axis on USG
2. Painful lymph nodes.
3. Patients with contraindications for MR examination.
4. Patients not willing to participate in the study

Results: In our study we found that the range of ADC values for tuberculous cervical lymph nodes was between $0.99-1.01 \times 10^{-3} \text{mm}^2/\text{s}$ in the solid portion of the lymph node and $1.27 - 1.31 \times 10^{-3} \text{mm}^2/\text{s}$ in the necrotic portion of the lymph node. The mean of ADC values for malignant (metastatic) cervical lymph nodes was between $0.78 - 0.87 \times 10^{-3} \text{mm}^2/\text{s}$ in the solid portion and in the necrotic portion the values were ranging from $1.94 - 2.0 \times 10^{-3} \text{mm}^2/\text{s}$. The sensitivity was 98.5% and the specificity was 98.3% and the accuracy was 98%. The „p” value was <0.001 , this showed that there is good agreement between the ADC values and the histopathology results.

Conclusions: The ADC values both of the necrotic and solid portions of the lymph nodes are useful in differentiation between the causes of cervical lymphadenopathy. The ADC value of necrosis is especially helpful in discriminating metastasis from tuberculosis.

Keywords: DWI, ADC value, solid and necrotic portion of lymph nodes.

Introduction

Modern imaging modalities such as ultrasound, computed tomography and magnetic resonance imaging allow reliable detection of cervical lymph nodes. However, the differentiation of benign and malignant lymph nodes remains very challenging. In addition to a size of more than 10mms, morphological criteria such as rounded shape, regional grouping of lymph nodes, and presence of necrosis, extra capsular tumor spread or the invasion of adjacent structures are indicative of malignancy. Unfortunately, none of these criteria is absolutely reliable. Several reports showed that these parameters are not enough to discriminate benign from malignant lymph nodes. The size is certainly the most used criterion for the diagnosis, whereas the presence of central necrosis is the most reliable criterion of malignancy. Lymph nodes maybe enlarged reactively and even small lymph nodes may be infiltrated by malignant cells. Presence of necrosis is the strongest indicator for malignancy, but necrosis has been shown to occur in benign conditions as well.^[1-6]

Alternative imaging modalities such as single photon emission computed tomography (SPECT) and positron emission tomography (PET) can help to differentiate between benign and malignant lymph nodes. However, these methods are invasive, expensive, time consuming and hampered by limited spatial resolution.^[7]

Ultrasound guided fine needle aspiration cytology (USgFNAC) is a valuable tool in characterizing cervical lymph nodes, but the method is invasive and operator dependent.^[8]

Whereas conventional MR sequences do not seem to be superior to CT. Nowadays the newer MRI technique of diffusion weighted imaging (DWI) and apparent diffusion coefficient mapping [ADC mapping], is used which is a non-invasive MRI technique. It is based on intra voxel incoherent motions imaging and allows visualization of diffusion properties of water molecules in biologic tissues. It provides image contrast dependent on the molecular motions of water. Any architectural changes in the proportion of intracellular and extracellular water protons will alter the diffusion coefficient of the tissue. Therefore, DWI would help in characterization of different tissues and lesions.^[9,10]

Anatomy

Surgical classification of cervical lymph nodes

The most recent American Head and Neck Society (AHNS) and American Academy of Otolaryngology Head and Neck Surgery have developed a widely accepted division of cervical lymph nodes into 7 numbered nodal levels with well defined anatomic boundaries that can be easily identified by both surgeons and radiologists. (Table 1).^[15-22]

Table 1: The cervical lymph nodes levels

Levels	Sublevels	Nodes
Level I	I A	Submental nodes
	I B	Submandibular nodes
Level II	II A	Antero-inferior upper jugular nodes
	II B	Postero-superior upper jugular nodes
Level III		Middle jugular nodes
Level IV		Lower jugular nodes
Level V	V A	Superior posterior neck nodes
	V B	Inferior posterior neck nodes
Level VI		Central (anterior) nodes
Level VII		Superior mediastinal nodes

Magnetic Resonance Imaging (MRI)

MRI is a modality with no hazard from ionizing radiation and it with its high contrast resolution and multiplanar imaging capabilities readily

detects abnormal lymph nodes and modern turbo spin echo sequences have helped shorten the examination time. MRI has added value in evaluating a primary neo plastic process, with

improved detection of bone marrow involvement and perineural spread of disease. The role of contrast-enhanced imaging in MRI is well established. Gadolinium contrast media is integral to the evaluation of cervical lymph nodes by MRI in evaluating for nodal necrosis and in evaluating characteristics of the primary lesion such as perineural spread of malignancy. Perfusion techniques evaluate dynamic microscopic blood flow changes by documenting changes in signal intensity in a given region of interest after bolus administration of contrast material. These techniques are non-invasive and can be obtained without adding significant additional time to imaging protocols. Recent studies of dynamic susceptibility weighted perfusion MRI have shown promise in differentiating metastasis from benign lymph nodes.^[23,24,33]

Diffusion weighted imaging (DWI)

Restricted diffusion

DWI is a non-invasive imaging technique, which probes the physical structure of a biologic tissue. DWI reveals insight into the morphologic composition of a tissue well below the typical millimeter-scale resolution of other imaging techniques. DWI exploits the random motions of water in the targeted tissue which reflects the tissue specific diffusion capacity. Thus the diffusion capacity can be used for tissue characterization.^[25-30] In water free diffusivity is present and water molecules show unrestricted diffusion. In biologic tissues the diffusivity of water molecules is confined by the intracellular and extracellular spaces. Rapidly growing malignant tumors are composed of layers of densely packed tumor cells with high energy turnover. These tumor cells present with enlarged nuclei, increased numbers of intracellular organelles and reduced cytoplasm. As a consequence the dimensions of both the intracellular and the extracellular spaces are reduced, resulting in decreased mobility of water protons and consequently a restricted diffusion capacity of the tissue. The signal on DWI derived

from diffusion sensitized water protons which show translational motions along the applied diffusion gradient. In a tissue with restricted diffusion capacity such as in tumor tissues the mobility of diffusion sensitized water protons is decreased resulting in increased signals on DWI. Thus, tumors present with bright signals on DWI.^[31,35-37]

Benign tissues are in general composed of loosely attached cells with small nuclei and increased amounts of cytoplasm resulting in enlarged intracellular and extracellular spaces. In these tissues the diffusion capacity is not restricted and diffusion sensitized water protons show increased translational motions along the applied diffusion gradient. This motion results in a phase shift of the sensitized water protons and consecutively in a signal loss on DWI.^[31,35,38]

According to this concept the contrast on DWI reflects the different diffusion capacities of the tissues under investigation. Malignancies appear hyperintense on DWI whereas benign tissues and liquids appear hypointense. This concept of restricted diffusion in tumor tissues has been derived from theoretical and biological diffusion models and has been supported by results from animal studies and human trials.^[31,32,36,37,28 -41]

DWI and lymph nodes

DWI is a well established imaging modality for the central nervous system (CNS). Its use for tissues outside the brain was limited for a long time because the image quality of non-CNS tissue was impaired by motion artifacts and challenging magnetic environment. Advances in the DWI software and in the hardware of MRI scanners improved image quality considerably and led to several reports describing the potential of DWI in the evaluation of non-CNS tissue. First reports described the power of DWI in the evaluation of bone marrow alterations in the spine. The contrast on DWI allowed the differentiation of benign from pathologic bone marrow alterations supporting the concept of restricted diffusion in tumor tissue. In the routine work-up of patients

with compression fractures of vertebral bodies DWI provides reliable information to distinguish pathologic from osteoporotic fractures. Knowledge gained from these studies was used to solve the problems in distinguishing metastatic lymph nodes from reactive ones. First results were obtained from lymph nodes of the head and neck region using a navigated diffusion weighted echo planar imaging (DW-EPI) with b factor values of 0 s/mm² and 800 s/mm². Regular lymph nodes showed ADC value of $1.21 \pm 0.24 \times 10^{-3} \text{ mm}^2/\text{s}$ which was significantly higher than the diffusivity of metastatic lymph nodes (ADC value: $0.59 \pm 0.27 \times 10^{-3} \text{ mm}^2/\text{s}$). Similar results were published by other authors also^[35-38].

b-factor value

The term b-factor value refers to the strength of the diffusion sensitizing gradient which is proportional to the gradient amplitude, the duration of the applied gradient and the time interval between paired gradients. It is measured in seconds per square millimetre (s/mm²). The b-factor value has to be determined by the

specifications of the MR scanner and the image quality. As has been shown in previous studies which described the role of DWI in the evaluation of musculoskeletal (MSK) pathologies, a b-factor value of 800s/mm² provides good image quality in respect to signal to noise ratio (SNR), acquisition time and spatial resolution. DWI obtained with lower b-values (less than 150 s/mm²) will have higher SNR however, the ADC values may be falsified by signals from perfusion in small vessels, so called pseudo diffusion. Using higher b-factor values may improve the specificity of the contrast on DWI, however, lower signal SNR and increased susceptibility artifacts have to be traded in which will impair image quality and the accuracy of qualitative image analysis. There is no unique b-factor value established for DWI of lymph nodes yet. b-factor values are dependent on the hardware components of the scanner and the applied software used, which will be different for each site. Thus the appropriate b-factor value has to be evaluated for each scanner/coil system and the specific DW sequence used. (Figure 12 and 13).^[33, 38-40]

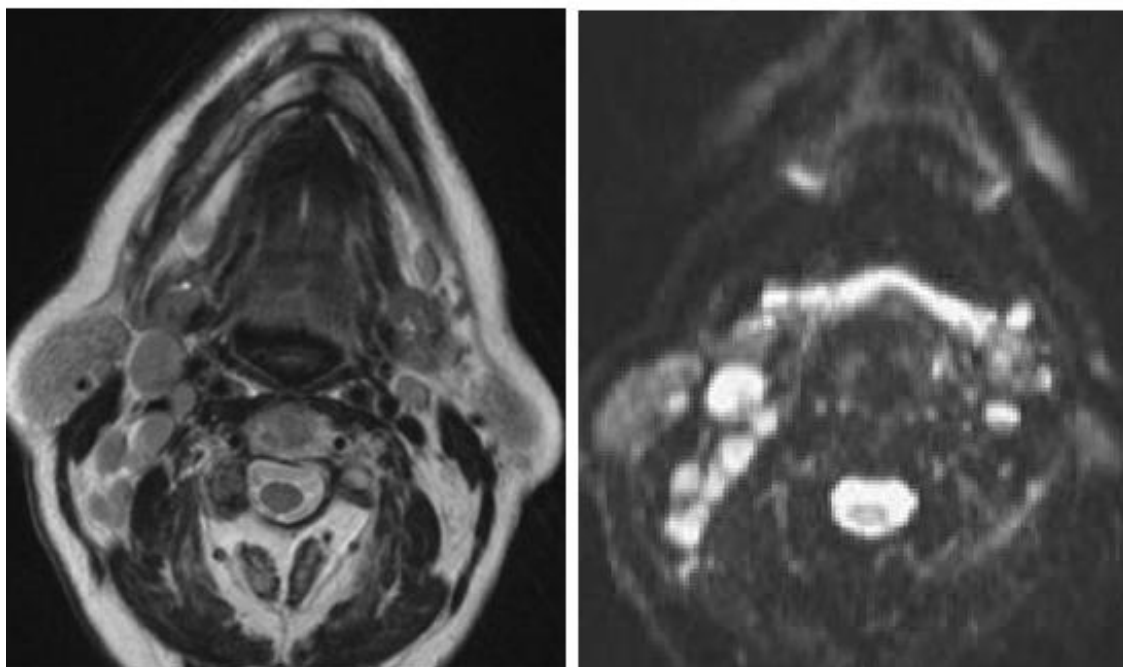


Figure 1: Metastatic cervical lymph nodes; First image: Axial fat suppressed T2 weighted MRI showing bilateral abnormal level II lymph nodes. Second image: Axial diffusion-weighted image obtained showing high signal intensities, showed b value = $0.79 \times 10^{-3} \text{ s/mm}^2$ seen in the solid portion in the lymph nodes.

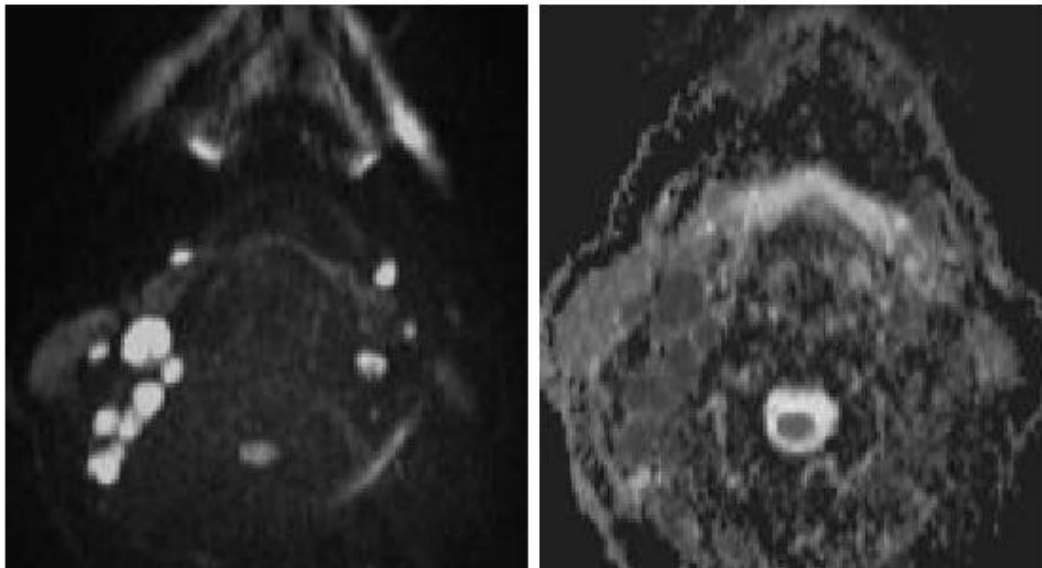


Figure 2: Metastatic cervical lymph nodes; First image: Axial diffusion-weighted image obtained showing high signal intensities, shows b value = 0.98×10^{-3} s/mm² seen in the necrotic portion of the lymph node. ; Second image: Corresponding areas are hypointense on the ADC map.

Histopathology

It is the gold standard, and is considered the best for arriving at a particular diagnosis. Tissue diagnosis gives the most accurate results with a sensitivity and specificity of close to 100 %. Although it is an accurate method but is invasive and operator dependent with high incidence of false negative case. But it has shown importance in certain cases wherein there is overlapping of the disease like for example a patient having an underlying malignancy gets superimposed with tuberculous infection due to his immune-compromised status, where other imaging modalities have difficulty in differentiating the same.[Figure 14,15,16].



Figure 3:-Z-N stain for mycobacteria showed the presence of numerous granulomas characterized

by central caseous necrosis, surrounded by a zone of epithelioid macrophages. There are scattered Langerhan's giant cells with multiple nuclei arranged in a peripheral pattern. The small round cells represent lymphocytes.

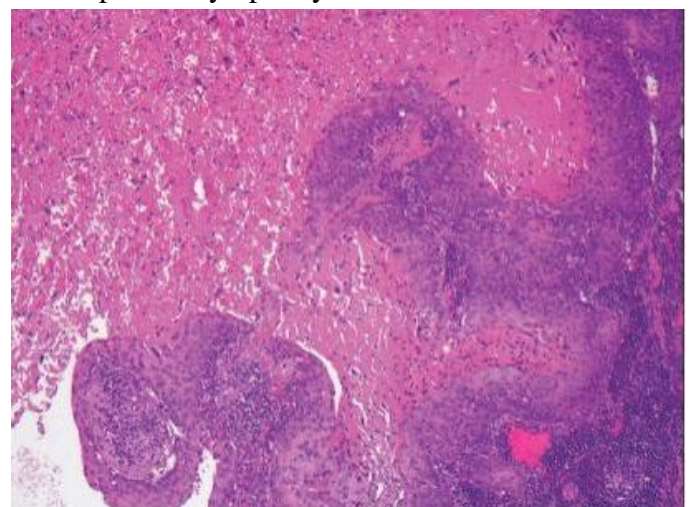


Figure 4:- Histopathology slide of metastatic squamous cell carcinoma to cervical lymph node with extensive tumor necrosis (H and E, $\times 100$)



Figure 5: Neck ultrasound image showing an enlarged, rounded, hypoechoic lymph node characteristic of malignancy, undergoing fine needle aspiration with a 21-gauge needle (*indicates needle tip).

Observations and Results

The present study “The potential role of apparent diffusion coefficient values in the differentiation of tuberculous and malignant lymph nodes of neck - in correlation with histopathology.”, was carried out from January 2015 to December 2015, in the department of Radiodiagnosis at our hospital which is a tertiary care centre in Southern parts of India. 40 patients having cervical lymphadenopathy were included in the study.

Table 2: MRI Diagnosis with Histopathologic Correlation

Cross tabulation Summary of Mridiagnosis V/S Histopathology diagnosis

			Histopathology Diagnosis			Total
			Infective etiology	Neoplastic	Tuberculous	Total
MRI diagnosis	Neoplastic	Count	1	18	0	19
		% within Histopathology Diagnosis	7.1%	100.0%	.0%	32.2%
	Tuberculous	Count	0	0	27	27
		% within Histopathology Diagnosis	.0%	.0%	100.0%	45.8%
Total		Count	14	18	27	46
		% within Histopathology Diagnosis	100.0%	100.0%	100.0%	100.0%

Table 2 shows that amongst all the cases studied MRI gave a diagnosis of infective etiology in 13 of the 13 cases which were given on histopathology

which corresponded to 100%. 27 patients were given a diagnosis of tuberculosis on MRI and histopathology, which showed 100 % correlation.

Table 3: MRI Diagnosis of Lymphnode

Diagnosis	Frequency	Percentage
Neoplastic	19	41%
Tuberculous	27	59%
Total	46	100%

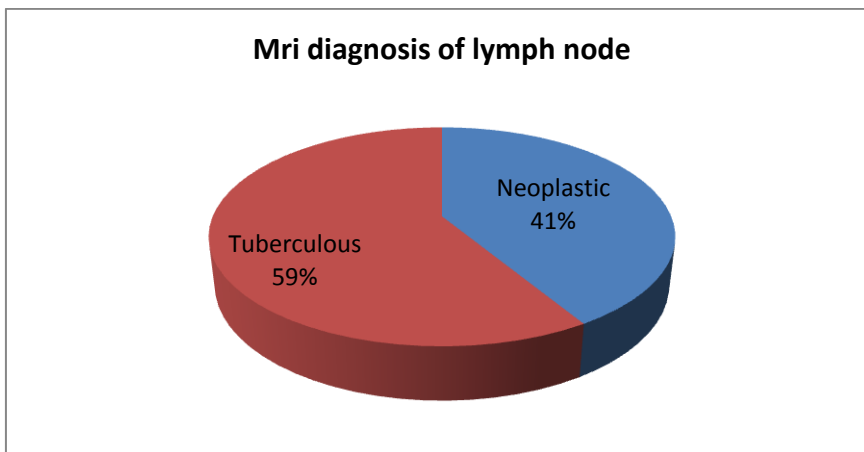


Table 4: Histopathology Diagnosis of Lymphnode

Diagnosis	Frequency	Percentage
Infective	1	2.1%
Neoplastic	18	39.1%
Tuberculous	27	58.8%
Total	46	100%

Table 5: MRI Diagnosis with Histopathology Correlation

	MRI diagnosis	histopathology diagnosis
Infective	0	1
Neoplastic	19	18
Tuberculous	27	27
Total	46	46

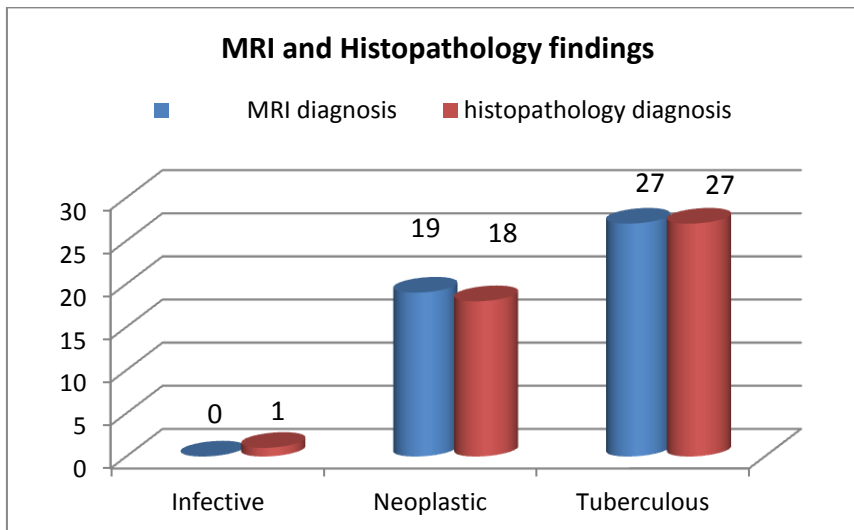


Table 6: Chi-Square Analysis of MRI With Histopathology

	Value	df	Asymp. Sig. (2-sided)
Pearson Chi-Square	110.902(a)	4	.000
Likelihood Ratio	117.392	4	.000
N of Valid Cases	40		

a 3 cells (33.3%) have expected count less than 5. The minimum expected count is 3.08. The cross tabulations study showed that there is strong association of MRI with histopathology with a 'P' value of 0.00 [P value of < 0.05 strong association] In the total number of patients studied (46) there was a mismatch in the diagnosis of 1 patient on

MRI and histopathology. MRI gave a total of 19 patients as having malignancy (metastatic lymphadenopathy) whereas the actual number of patients having malignancy or metastasis was 18 according to histopathology. This was the grey zone in the diagnosis of MRI where it was not able to differentiate between the lymph nodes .

Table 8: ADC in Differentiation of Infective Lymph Nodes

ADC($\times 10^3$ mm ² /s) of solid portion	of	ADC($\times 10^3$ mm ² /s) of necrotic portion	MRI diagnosis	Histopathological diagnosis
1.0 – 1.2		No necrosis	Infective etiology	Infective etiology

Table 9: ADC in Differentiation of Tuberculous Lymph Nodes

ADC($\times 10^3$ mm ² /s) of solid portion	of	ADC($\times 10^3$ mm ² /s) of necrotic portion	MRI diagnosis	Histopathological diagnosis
0.99 – 1.01		1.27-1.31	TB	TB

Table 10: ADC in Differentiation of Malignant Lymph Nodes

ADC($\times 10^3$ mm ² /s) of solid portion	of	ADC($\times 10^3$ mm ² /s) of necrotic portion	MRI diagnosis	Histopathological diagnosis
0.78-0.87		1.94 – 2.0	Malignant	Malignant

Table 11: ADC in Correctly Identifying Malignant Lymph Nodes

ADC	No of Patients	Percentage
Correct	18	98.30 %
Incorrect	1	1.69 %
Total	19	100%

All ADC values were corresponding with the histopathology except in one patient wherein MRI diagnosis was made as Malignant but the histopathological diagnosis was of Infective etiology. We can thus see that MRI [ADC values] is having 98.3 % sensitivity and 99% specificity as compared to histopathology, which showed 100 % sensitivity, and specificity in correctly diagnosing cervical lymphadenopathies. The „p“ value was <0.001 which showed that ADC values are highly significant in the differentiation of benign and malignant lymph nodes. This showed that there is good agreement between the ADC values and the histopathology results. The interpretation of DWI in such a complex area as the head and neck is not straightforward, requiring training and experience. Reproducing

these promising results on a broad scale will be a challenge, and technique standardisation is desirable. For example, the results obtained are very dependent on the selection of the *b*-values. Also other technical issues, such as magnetic field inhomogeneity or suboptimal placement of receiver coils, have a strong negative effect on image quality. All the mentioned studies in literature were giving only one value in the lymph node. They were not differentiating between the solid and necrotic portion. In our study we found that the range of ADC values for benign cervical lymph nodes in the solid and necrotic portion was different as compared to the values seen in the malignant nodes.. The sensitivity was 98.5% and the specificity was 98.3% and the accuracy was 98%.

The „p“ value was <0.001, which showed that the ADC values are highly significant in the differentiation of benign and malignant lymph nodes of neck. The „k“ value was 0.9. This showed that there is good agreement between the ADC values and the histopathology results.

Therefore, although most radiologists emphasize that these techniques are very accurate, most clinicians have maintained that none of these techniques is perfect and thus refrain from adjusting their management policy in individual cases according to the outcome of these imaging modalities. Currently there are compelling clinical and pharmaceutical needs to move towards an ideal diagnostic imaging technique able to assess the cancer burden avoiding radiation exposure and to fulfill some essential prerequisites: accuracy, availability, reproducibility, cost effectiveness, and efficiency. DWI seems to fulfill these requirements, because no ionizing radiation is administered and no intravenous injection of isotopes or any contrast medium is necessary.

Discussion

The objective of the study is to determine the accuracy of MRI [DWI/ADC] in differentiating between benign and malignant enlarged cervical lymph nodes.

In our study we surveyed a total of 65 patients with cervical lymphadenopathy. Of these 59 patients underwent FNAC and were included in the study. The 5 patients for whom FNAC could not be done were excluded from the study.

In the 59 patients we have seen, we were able to formulate a range of ADC values within which if the lymph nodes fell we have categorized them as benign or malignant.

The maximum number of patients was seen in the age group of 31 -40 years with maximum age of 81 and a minimum age of 22 years .We found that there was no particular predilection of the nature of the lymphadenopathy to the age of the patient.

Amongst the patients studied, 15 patients had few (≤ 10) lymph nodes involved (25.4%) and 44 patients had multiple (>10) lymph nodes

involvement (74.5%). We tried to find a correlation between the multiplicity of the lymph nodes and the benign or malignant nature of the disease. It was seen that the ‘p’ value was 0.022 which showed that there was moderately significant correlation.

Amongst the patients studied, 11 had largest lymph node sizes between 1.1 - 2.0cms, 26 had largest lymph node sizes of 2.1-3.0cms and 22 had largest lymph node sizes of > 3.1 cm. Mean of largest lymph node sizes of benign lymph nodes was 2.4cms with a standard deviation of 0.2, median of largest lymph node sizes of benign lymph nodes was 2.5 cms and range of largest lymph node sizes of benign lymph nodes was 1.9-2.8cms. Mean of largest lymph node sizes of malignant lymph nodes was 2.7cms with a standard deviation of 0.5, median of largest lymph node sizes of malignant lymph nodes was 2.8cms and range of largest lymph node sizes of malignant lymph nodes was 1.8-3.6cms. It was seen that there was no particular correlation between the lymph node size and the nature of the lymph node.

In our study we saw that 12 patients had unilateral lymph nodes [33.9%] while bilateral lymph nodes were seen in 47 of the patients [66.1%] (table 5). There was no particular disease predilection for unilaterality or bilaterality of the lymph nodes.

Amongst the total number of cases studied 43 patients had lymph nodes with necrosis [72.9%] whereas 16 patients had lymph nodes without necrosis [27.9%].

On ultrasonography amongst the patients studied 43 patients showed signs of necrosis (27.1%) and no necrosis was seen in 16 patients (72.9%). Of the 43 lymph nodes with necrosis MRI showed lower ADC values in 19 which were proven to be malignant.

Bondt et al.^[8] reported that the ADC values of malignant cervical lymph nodes were significantly lower compared with benign cervical lymph nodes with mean values of $0.85 \times 10^{-3} \text{mm}^2/\text{s}$ and $1.2 \times 10^{-3} \text{mm}^2/\text{s}$ respectively. He also stated that the optimal ADC threshold value for the diagnosis

of malignant cervical lymph nodes was $1.0 \times 10^{-3} \text{mm}^2/\text{s}$ with sensitivity, specificity, positive predictive value (PPV) and negative predictive value (NPV) of 92.3%, 83.9%, 43.6% and 98.8% respectively.

Our study showed similar correlation where the mean ADC values seen in malignant cervical lymph nodes were $0.87 \times 10^{-3} \text{mm}^2/\text{s}$ and in benign cervical lymph nodes were $1.27 \times 10^{-3} \text{mm}^2/\text{s}$.

Amongst all the cases MRI showed higher ADC values in 40 patients with enlarged cervical lymphadenopathy which were proven to be benign in nature. In our study the mean ADC value in benign cervical lymphadenopathy was $1.27 \times 10^{-3} \text{mm}^2/\text{s}$

Perrone et al. showed that the mean ADC value of benign lymph nodes was $1.44 \times 10^{-3} \text{mm}^2/\text{s}$ and of malignant (metastatic) cervical lymph nodes was $0.85 \times 10^{-3} \text{mm}^2/\text{s}$. He thus concluded that the ADC value of benign cervical lymph nodes was higher than those of malignant. The best threshold value for differentiating malignant from benign nodes was $1.03 \times 10^{-3} \text{mm}^2/\text{s}$ obtaining a sensitivity of 100% and a specificity of 92.9%.

Our study showed similar correlation with the above study, wherein the ADC values for benign lymph nodes was comparatively higher than for malignant lymph nodes.

On MRI 19 patients had a ADC value between $0.78-0.87 \times 10^{-3} \text{mm}^2/\text{s}$ favouring malignancy (metastatic lymphadenopathy) whereas the actual number of patients having malignancy according to histopathology was 18. This discrepancy was seen as the cervical lymph node had both areas of necrosis and solid component. An ADC value was taken from both these areas which was lower ($0.78 - 0.87$). This was the grey zone in the diagnosis of MRI where it was not able to differentiate between the lymph nodes. We did not find any relevance in literature as to the reason of our discrepancy.

As there was no incidence of necrosis in infective lymph nodes only a single value was taken. ADC mapping showed that the lymph nodes whose

values were between 1.0 and 1.2 were found to be of infective nature on histopathology. The only exception was the one case which was misdiagnosed by MRI as it showed lower ADC values in comparison with the other infective cases.

Chang et al. reported an ADC threshold value of $1.22 \times 10^{-3} \text{mm}^2/\text{s}$, with a sensitivity of 91% and a specificity of 93% for differentiation of benign and malignant lymph nodes of neck. Our study showed similar correlation with the above study, wherein the ADC values for benign lymph nodes was comparatively higher than for malignant lymph nodes.

Sumi et al. reported that the ADC was significantly greater in metastatic cervical lymph nodes ($(0.410 \pm 0.105) \times 10^{-3} \text{mm}^2/\text{s}$) than in benign cervical lymph nodes ($(0.302 \pm 0.062) \times 10^{-3} \text{mm}^2/\text{s}$). Lymphomas showed even lower levels of ADC ($(0.223 \pm 0.056) \times 10^{-3} \text{mm}^2/\text{s}$). This may be because 48% of their metastatic cervical lymph nodes had central necrosis resulting in a large variability in the ADC values of these nodes.

Sumi et al. found that the ADC of metastatic cervical lymph nodes ($(1.167 \pm 0.447) \times 10^{-3} \text{mm}^2/\text{s}$) was significantly higher than that of benign cervical lymph nodes ($(0.652 \pm 0.101) \times 10^{-3} \text{mm}^2/\text{s}$) and that of lymphomas ($(0.601 \pm 0.427) \times 10^{-3} \text{mm}^2/\text{s}$). The ADC of lymphomas was significantly lower than that of the benign cervical nodes. They might have found higher ADC values in metastatic cervical lymph nodes since they did not analyze necrotic and solid parts of lymph nodes separately. ADC values measured in necrotic areas were high in Holzapfel et al. study ($1.98 \times 10^{-3} \text{mm}^2/\text{s}$) and in Razek et al. study ($1.96 \times 10^{-3} \text{mm}^2/\text{s}$).

Tamer F. Taha Ali et al reported in his study that the mean ADC values of benign, metastatic and lymphomatous neck nodes were $(1.51 \pm 0.36) \times 10^{-3} \text{mm}^2/\text{s}$, $(0.92 \pm 0.13) \times 10^{-3} \text{mm}^2/\text{s}$ and $(0.74 \pm 0.14) \times 10^{-3} \text{mm}^2/\text{s}$ respectively. The ADC values of the benign neck lymph nodes were significantly higher than those of metastatic nodes

and lymphoma. Furthermore, the ADC values of the metastatic neck lymph nodes were significantly higher than those of lymphoma. The best ADC threshold value for differentiating benign and malignant lymph nodes was $1.15 \times 10^{-3} \text{mm}^2/\text{s}$ with sensitivity, specificity, positive predictive value (PPV), negative predictive value (NPV), „p“ value and „κ“ value 96%, 88.9%, 96%, 88.9%, 0.84 and <0.0001 respectively.

Two values were taken in each lymph node. One from the necrotic portion and one from the solid portion of the lymph node. On MRI/ADC mapping, lymph nodes whose values were between 0.99 – 1.01 in the solid portion and 1.27 - 1.31 in the necrotic portion were given a diagnosis of tuberculous lymphadenitis. This corresponded to a total of 27 patients who were also given a diagnosis of TB lymphadenitis / granulomatous lymphadenitis on histopathology. Thus MRI showed 100% correlation with histopathology in diagnosing tuberculous lymphadenopathy.

Two values were taken in each lymph node. One from the necrotic portion and one from the solid portion of the lymph node. On MRI/ADC mapping, lymph nodes whose values were between 0.78 – 0.87 in the solid portion and 1.94 – 2.0 in the necrotic portion were given a diagnosis of malignant/ metastasis on MRI. Of 19 patients diagnosed as malignant on MRI, 18 patients were histopathologically proven to be malignant. This difference in the results was due to the presence of necrosis and the lower ADC values obtained in the patient who actually presented with infective etiology. These nodes did not show any malignant potential but were purely infective on histopathology.

Holzappel et al. in their study found that the mean ADC value of malignant (metastatic and lymphomatous) cervical lymph nodes was $(0.74 \pm 0.11) \times 10^{-3} \text{mm}^2/\text{s}$. ADC values of metastatic lymph nodes ranged between $0.62 \times 10^{-3} \text{mm}^2/\text{s}$ and $0.93 \times 10^{-3} \text{mm}^2/\text{s}$ with a mean ADC value of $(0.78 \pm 0.09) \times 10^{-3} \text{mm}^2/\text{s}$. ADC values of lymphomatous nodes ranged

between $0.51 \times 10^{-3} \text{mm}^2/\text{s}$ and $0.76 \times 10^{-3} \text{mm}^2/\text{s}$ with a mean ADC value of $(0.64 \pm 0.09) \times 10^{-3} \text{mm}^2/\text{s}$. ADC values of benign lymph nodes ranged between $0.84 \times 10^{-3} \text{mm}^2/\text{s}$ and $1.47 \times 10^{-3} \text{mm}^2/\text{s}$ with a mean ADC value of $(1.24 \pm 0.16) \times 10^{-3} \text{mm}^2/\text{s}$. The optimal threshold ADC value for differentiating between benign and malignant cervical lymph nodes determined by receiver operating characteristic (ROC) curve analysis was $1.02 \times 10^{-3} \text{mm}^2/\text{s}$ which resulted in a sensitivity of 100%, a specificity of 87.0%, an accuracy of 94.3%, a positive predictive value (PPV) of 90.9% and a negative predictive value (NPV) of 100%.

Barchetti et al. found that in the 412 histologically confirmed benign lymph nodes of neck the mean ADC value was $1.650 \times 10^{-3} \text{mm}^2/\text{s}$ (range: $0.945\text{-}2.370 \times 10^{-3} \text{mm}^2/\text{s}$) and in the 239 histologically proven metastatic lymph nodes of neck the mean ADC value was $0.903 \times 10^{-3} \text{mm}^2/\text{s}$ (range: $0.400\text{-}0.996 \times 10^{-3} \text{mm}^2/\text{s}$). The most reliable threshold of ADC value derived from the receiver operating characteristic (ROC) curve analysis for differentiating benign and metastatic lymph nodes of neck was $0.965 \times 10^{-3} \text{mm}^2/\text{s}$ which was showing sensitivity of 97% , specificity of 93%, accuracy of 92%, positive predictive value (PPV) of 95%, and negative predictive value (NPV) of 96%.

Razek et al. reported that the mean ADC value of metastatic $(1.09 \pm 0.11) \times 10^{-3} \text{mm}^2/\text{s}$ and lymphomatous $(0.97 \pm 0.27) \times 10^{-3} \text{mm}^2/\text{s}$ cervical lymph nodes was significantly lower than that of benign $(1.64 \pm 0.16) \times 10^{-3} \text{mm}^2/\text{s}$ cervical lymph nodes. When an ADC value of $1.38 \times 10^{-3} \text{mm}^2/\text{s}$ was used as a threshold value for differentiating benign and malignant lymph nodes, the results obtained were a sensitivity of 98%, a specificity of 88%, an accuracy of 96%, a positive predictive value (PPV) of 98.5% and a negative predictive value (NPV) of 83.7%.

King et al. found that by using data from a single section through a cervical node with exclusion of any areas of necrosis the mean apparent diffusion coefficient (ADC) value for squamous cell

carcinoma (SCC) was $1.057 \times 10^{-3} \text{mm}^2/\text{sec}$ greater than that for nasopharyngeal carcinoma (NPC) ($0.802 \times 10^{-3} \text{mm}^2/\text{sec}$) and that for lymphoma ($0.664 \times 10^{-3} \text{mm}^2/\text{sec}$).

The ADC values were corresponding with the histopathology in all patients except one. In this patient there was solid and necrotic components in the lymph node along with a low ADC value hence a diagnosis of metastasis/ malignancy was proposed. Thus in our study we saw MRI [ADC values] having 98.3 % sensitivity and 99% specificity as compared to histopathology, which showed 100 % sensitivity, and specificity in correctly diagnosing cervical lymphadenopathies. The „p“ value was <0.001 which showed that ADC values are highly significant in the differentiation of benign and malignant lymph nodes.

Limitations of the study

In our study we did not correlate the possibility of necrotic lymph nodes with extracapsular spread, which if correlated we could have had more insight into the disease process.

As we had majority of the cases with squamous cell carcinoma we have limited experience in the characteristics shown by lymphoma.

Newer Techniques and possibilities

Recent advances in iron oxide nanocrystal technology [SPIO and USPIO] along with T1WI and T2*WI for medical imaging plays an important role for angiography and detection of invasibility of the tumor/ lymph nodes.

FDG whole body PET/ MRI can be used to detect the spread of the disease.

Conclusion

In our study we found that the range of ADC values for benign cervical lymph nodes was between $0.99-1.03 \times 10^{-3} \text{mm}^2/\text{s}$ in the solid portion of the lymph node and $1.27 - 1.31 \times 10^{-3} \text{mm}^2/\text{s}$ in the necrotic portion of the lymph node. The mean of ADC values for malignant (metastatic) cervical lymph nodes was between

$0.78 - 0.87 \times 10^{-3} \text{mm}^2/\text{s}$ in the solid portion and in the necrotic portion the values were ranging from $1.94 - 2.0 \times 10^{-3} \text{mm}^2/\text{s}$. The sensitivity was 98.5% and the specificity was 98.3% and the accuracy was 98%. The „p“ value was <0.001 , this showed that there is good agreement between the ADC values and the histopathology results.

Hence findings of our study and other studies quoted above suggest that the ADC values can well be used in the differentiation of tuberculous and malignant lymph nodes of neck.

Bibliography

1. Koc, O, Paksoy Y, Erayman I, Kivrak AS, Arbag H. Role of diffusion weighted MR in the discrimination diagnosis of the cystic and/or necrotic head and neck lesions. *Eur J Radiol* 2007;62:205-213.
2. Castelijns JA, van den Brekel MW. Imaging of lymphadenopathy in the neck. *Eur Radiol* 2002;12:727-738.
3. King AD, Tse GM, Ahuja AT, et al. Necrosis in metastatic neck nodes: Diagnostic accuracy of CT, MR imaging, and US. *Radiology* 2004;230:720-726.
4. Van den Brekel MW, Castelijns JA, Snow GB. The size of lymph nodes in the neck on sonograms as a radiologic criteria for metastasis: How reliable is it? *AJNR Am J Neuroradiol* 1998;19(4):695-700.
5. Van den Brekel MW, Castelijns JA, Snow GB. Detection of lymph node metastases in the neck, radiologic criteria. *Radiology* 1994;192(3):617-618.
6. Curtin HD, Ishwaran H, Mancuso AA, Dalley RW, Caudry DJ, McNeil BJ (1998) Comparison of CT and MR imaging in staging of neck metastases. *Radiology* 207:123-130.
7. Veit P, Ruehm S, Kuehl H, et al. Lymph node staging with dual-modality PET/CT: Enhancing the diagnostic accuracy in oncology. *Eur J Radiol* 2006;58:383-389.
8. De Bondt RB, Nelemans PJ, Hofman PA, et al. Detection of lymph node metastases

- in head and neck cancer: A meta-analysis comparing US, USgFNAC, CT and MR imaging. *Eur J Radiol* 2007;64:266-272.
9. Le Bihan D, Breton E, Lallemand D, Aubin ML, Vignaud J, Laval-Jeantet M. Separation of diffusion and perfusion in intravoxel incoherent motion MR imaging. *Radiology* 1988;168:497-505.
 10. Herneth AM, Guccione S, Bednarski M. Apparent diffusion coefficient: A quantitative parameter for in vivo tumor characterization. *Eur J Radiol* 2003;45:208-213.
 11. Qizilbash AH, Young JEM, Eds. Lymph nodes. *Guides to Clinical Aspiration Biopsy: Head and Neck*. New York: Igaku-Shoin 1988;117203.
 12. Hall FG. The functional anatomy of lymph nodes. In Stansfeld AG, D'Ardenne AJ, eds. *Lymph Node Biopsy Interpretation*. London: Churchill Livingstone, 1992; 328.
 13. Castenholz A. Architecture of the lymph node with regard to its function. In Grundmann E, Vollmer E, eds. *Reaction Patterns of the Lymph Node. Part 1. Cell Types and Functions 1*. New York: SpringerVerlag, 1990;1-32.
 14. Papadimitriou CS, Kittas CN. Normal structure and function of lymph nodes. In Pangalis GA, Polliack A, eds. *Benign and malignant lymphadenopathies*. Chur: Harwood Academic Publishers, 1993;113-130.
 15. Rouvière H, Tobias MJ. *Anatomy of the human lymphatic system*. Ann Arbor (MI): Edwards brothers, inc; 1938. ix,318.
 16. Shah JP, et al. Surgical grand rounds. Neck dissection: current status and future possibilities. *Clin Bull* 1981;11(1):25-33.
 17. Robbins KT. Classification of neck dissection: Current concepts and future considerations. *Otolaryngol Clin North Am* 1998;31(4):639-655.
 18. Robbins KT, et al. Neck dissection classification update: revisions proposed by the American Head and Neck Society and the American Academy of Otolaryngology-Head and Neck Surgery. *Arch Otolaryngol Head Neck Surg* 2002;128(7):751-758.
 19. Som PM, Curtin HD, Mancuso AA. An imaging-based classification for the cervical nodes designed as an adjunct to recent clinically based nodal classifications. *Arch Otolaryngol Head Neck Surg* 1999;125(4):388-396.
 20. Robbins KT, et al. Consensus statement on the classification and terminology of neck dissection. *Arch Otolaryngol Head Neck Surg* 2008;134(5): 536-538.
 21. Vincent Chong. Cervical Lymphadenopathy: what radiologists need to know? *Cancer imaging (2004) 4*; 116-120.
 22. Sumi M, Sakihama N, Sumi T, Morikawa M, Uetani M, Kabasawa H et al. Discrimination of metastatic cervical lymph nodes with diffusion-weighted MR imaging in patients with head and neck cancer. *AJNR Am J Neuroradiol*. 2003 Sep;24(8):1627-34.
 23. Hudgins PA. Contrast enhancement in head and neck imaging. *Neuroimaging Clin North Am* 1994;4(1):101-115.
 24. Shah GV, et al. New directions in head and neck imaging. *J Surg Oncol* 2008;97(8):644-648.
 25. Zima A, et al. Can pretreatment CT perfusion predict response of advanced squamous cell carcinoma of the upper aerodigestive tract treated with induction chemotherapy? *AJNR Am J Neuroradiol* 2007;28(2):328-334.
 26. Bisdas S, et al. Quantitative measurements of perfusion and permeability of oropharyngeal and oral cavity cancer, recurrent disease, and associated lymph nodes using first-pass contrast-enhanced computed tomography studies. *Invest Radiol* 2007;42(3):172-179.

27. Abdel Razek AA, Gaballa G. Role of perfusion magnetic resonance imaging in cervical lymphadenopathy. *J Comput Assist Tomogr* 2011;35(1):21-25.
28. Le Bihan D, Turner R. Intravoxel incoherent motion imaging using spin echoes. *MagnReson Med* 1991;19(2):221-227.
29. Le Bihan D, et al. MR imaging of intravoxel incoherent motions: Application to diffusion and perfusion in neurologic disorders. *Radiology* 1986;161(2):401-417.
30. Turner R, et al. Echo-planar imaging of intravoxel incoherent motion. *Radiology* 1990;177(2):407-414.
31. Le Bihan DJ, Turner R. Diffusion and perfusion. In: Stark DD, Bradley WG, editors. *Magnetic resonance imaging*. St. Louis: Mosby; 1992;335.
32. Le Bihan D. Molecular diffusion, tissue microdynamics and microstructure. *NMR Biomed* 1995;8(7-8):375-386.
33. Herneth AM, Guccione S, Bednarski M. Apparent diffusion coefficient: A quantitative parameter for in vivo tumor characterization. *Eur J Radiol* 2003;45(3):208-213.
34. Lang P, et al. Osteogenic sarcoma: Noninvasive in vivo assessment of tumor necrosis with diffusion-weighted MR imaging. *Radiology* 1998;206(1):227-235.
35. Herneth AM, et al. Vertebral metastases: Assessment with apparent diffusion coefficient. *Radiology* 2002;225(3):889-894.
36. Latour LL, et al. Time-dependent diffusion of water in a biological model system. *ProcNatlAcadSci USA* 1994;91(4):1229-1233.
37. Le Bihan D, et al. Diffusion MR imaging: Clinical applications. *AJR Am J Roentgenol* 1992;159(3):591-599.
38. Le Bihan D, et al. Separation of diffusion and perfusion in intravoxel incoherent motion MR imaging. *Radiology* 1988;168(2):497-505.
39. Szafer A, et al. Diffusion-weighted imaging in tissues: Theoretical models. *NMR Biomed* 1995;8(7-8):289-296.
40. Carr H, Purcell E. Effects of diffusion on free precession in nuclear magnetic resonance experiments. *Phys Rev* 1954;94:630-635.
41. Conturo TE, et al. Diffusion MRI: Precision, accuracy and flow effects. *NMR Biomed* 1995;8(7-8):307-332.